PLANT SCIENCE

DNA replication–coupled histone modification maintains Polycomb gene silencing in plants

Danhua Jiang and Frédéric Berger*

Propagation of patterns of gene expression through the cell cycle requires prompt restoration of epigenetic marks after the twofold dilution caused by DNA replication. Here we show that the transcriptional repressive mark H3K27me3 (histone H3 lysine 27 trimethylation) is restored in replicating plant cells through DNA replication–coupled modification of histone variant H3.1. Plants evolved a mechanism for efficient K27 trimethylation on H3.1, which is essential for inheritance of the silencing memory from mother to daughter cells. We illustrate how this mechanism establishes H3K27me3-mediated silencing during the developmental transition to flowering. Our study reveals a mechanism responsible for transmission of H3K27me3 in plant cells through cell divisions, enabling H3K27me3 to function as an epigenetic mark.

Epigenetic marks participate in maintaining expression patterns from mother to daughter cells. During DNA replication, the passage of the replication fork disrupts chromatin structure (*1*). Maintenance of a stable pattern of transcription after DNA replication requires restoration of epigenetic marks in the G_2 phase soon after DNA replication. At replication sites, nucleosomes are assembled from recycled histones and newly synthesized, largely unmodified histones. In contrast to the histone H3 variant H3.3, the variant H3.1 is deposited at the replication fork by CAF1 (chromatin assembly factor 1) (*2*, *3*). Maintenance of transcriptional repressive states by histone H3 lysine 27 trimethylation (H3K27me3) deposited by Polycomb repressive complex 2 (PRC2) is a conserved mechanism in animals and plants (*4*, *5*), which involves positive-feedback loops (*6*–*9*). After DNA replication in mammalian cells, full levels of H3K27me3 are only restored at the next G_1 phase (*10*–*12*), likely as a result of the stepwise methylation of K27 by PRC2, from H3K27me1 during S phase to achieve H3K27me3 during the next G_1 phase (*10*–*14*).

In contrast to animals, plants evolved the PRC2-independent methyltransferases ATXR5 and ATXR6 (*ARABIDOPSIS* TRITHORAX-RELATED PROTEIN 5 and 6, hereafter referred to as ATXR5/6), which deposit H3K27me1 on H3.1 (*15*, *16*). Hence, the kinetics of H3K27me3 restoration might be different between plants and animals. To address this hypothesis, we synchronized the cell cycle of tobacco BY-2 cells (fig. S1, A and B) and measured total levels of H3K27me1 and H3K27me3. Levels of H3K27me1 were not reduced during S phase (Fig. 1A and fig. S1C), consistent with the association of ATXR5/6 at the replication fork (*15*). In contrast, levels of H3K27me3 dropped during S phase, likely reflecting the incorporation of newly synthesized, unmodified histones. Subsequently, H3K27me3 levels were restored early in G_2 phase and remained stable until the next G_1 phase (Fig. 1A and fig. S1C). These observations contrast with the slow restoration of H3K27me3 in animal cells, suggesting that plants have a specific mechanism dedicated to rapid restoration of H3K27me3 after DNA replication.

We hypothesized that the restoration of H3K27me3 depends on the incorporation of H3.1, the preferred substrate for monomethylation of K27 by ATXR5/6 (*15*). We first confirmed that *Arabidopsis* CAF1 deposits H3.1 (fig. S2). Next, in a yeast two-hybrid screen, we found that the conserved CAF1 subunit FASCIATA1 (FAS1) interacts with PRC2 and PRC1 components (fig. S3, A and B). In addition, FAS1 interacts with PCNA1/2 (proliferating cell nuclear antigens 1 and 2), which are associated with the DNA replication fork (fig. S3, A and C). We confirmed direct interactions of FAS1 with PCNA1/2, CLF (CURLY LEAF), LHP1 (LIKE HETEROCHROMATIN PROTEIN 1), and RING1A in vitro by pull-down assays and in vivo by co-immunoprecipitation (Co-IP) of functional proteins (Fig. 1, B and C, and fig. S3, D and E). Co-IP also supported interaction between LHP1 and PCNA1/2 (Fig. 1D). Consistent with these interactions, we observed significant colocalization of FAS1 and Polycomb group (PcG) proteins with DNA replication foci (fig. S4). Hence, PRC2 and PRC1 interact with CAF1 at DNA replication sites.

To elucidate whether the incorporation of H3.1 facilitates restoration of H3K27me3, we obtained H3.1-deficient plant lines. In *Arabidopsis*, H3.1 is encoded by five genes. We combined a *htr1; htr2;htr3;htr9* quadruple mutant with an artificial microRNA (amiRNA) targeting *HTR13* (*amiRHTR13-1* or *amiRHTR13-2*) and obtained two independent knockdown lines (*h3.1kd-1* and *h3.1kd-2*) that were largely deprived of H3.1 (fig. S5,

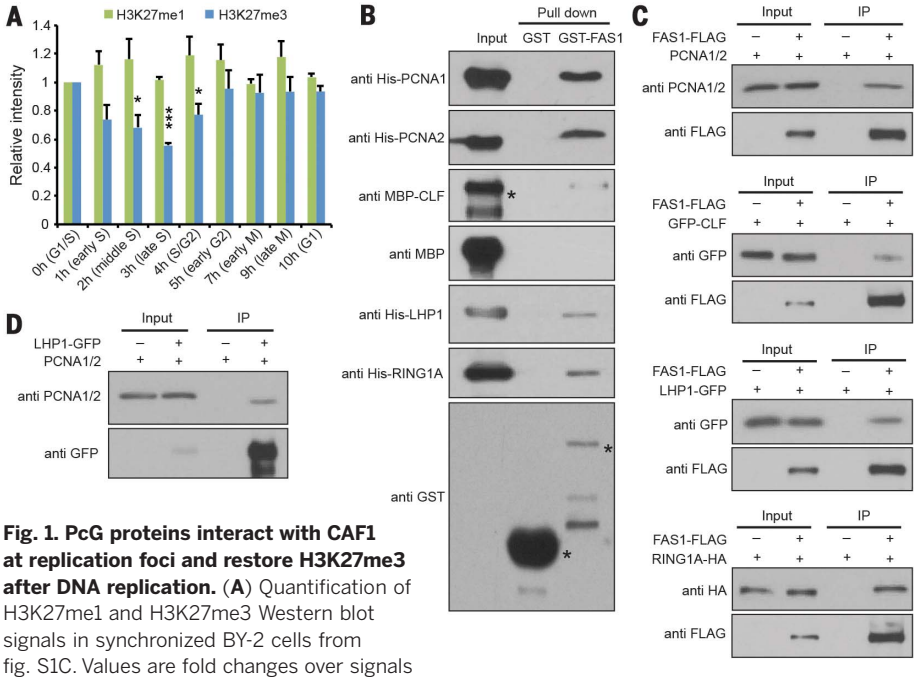

Fig. 1. PcG proteins interact with CAF1 at replication foci and restore H3K27me3 after DNA replication. (**A**) Quantification of H3K27me1 and H3K27me3 Western blot signals in synchronized BY-2 cells from fig. S1C. Values are fold changes over signals at 0 hours. Error bars represent SD from three biological replicates. Only H3K27me3 levels at 2, 3, and 4 hours are statistically different from those at 0 hours. Unpaired *t* test: $*P < 0.05$; $***P < 0.001$. (**B**) Protein pull-down assays of glutathione *S*-transferase (GST)–FAS1 with His-PCNA1/2, His-LHP1, His-RING1A, and maltose binding protein (MBP)–tagged CLF. Asterisks indicate full-length proteins. (**C**) Co-IP of FAS1 with PCNA1/2, CLF, LHP1, and RING1A. Plants not expressing FAS1-FLAG served as controls. GFP, green fluorescent protein; HA, hemagglutinin. (**D**) Co-IP of LHP1 with PCNA1/2. Wild-type Columbia (Col) accession served as control.

Gregor Mendel Institute, Austrian Academy of Sciences, Vienna Biocenter, Dr. Bohr-Gasse 3, 1030 Vienna, Austria.
***Corresponding author. Email: frederic.berger@gmi.oeaw.ac.at**

A and B). Plants from two *h3.1kd* lines showed similar developmental defects—including enlarged inflorescence meristems, fasciated stems, and ectopic leaflets—and produced shorter siliques (fig. S5C). These developmental defects could be rescued by expression of H3.1 (*HTR13r*, an *amiRNA* resistant *HTR13*) but not H3.3 (*HTR5*, an H3.3 coding gene), even when H3.3 was expressed under the control of the H3.1 promoter (fig. S5, D to G), highlighting the specific function of H3.1 in plant development.

We detected a reduction in the global levels of H3K27me1 and H3K27me3, but not H3K4me3, in *h3.1kd* lines (Fig. 2A and fig. S6A). To quantitatively profile H3K27me3 at chromatin, we employed chromatin immunoprecipitation with reference exogenous genome (ChIP-Rx) followed by DNA sequencing (*17*) and observed a genome-wide loss of H3K27me3 in *h3.1kd* lines, whereas the overall patterns of H3K27me3 were preserved (Fig. 2B and fig. S6, B to F). Moreover, genes up-regulated in *h3.1kd* lines were significantly overlapped with genes marked by H3K27me3 (Fig. 2C; fig. S7, A and B; and table S1) (*18*), including class I *KNOX* genes (*STM*, *KNAT1*, *KNAT2*, and *KNAT6*) that are involved in the activation of stem cells in the shoot meristem (Fig. 2D and fig. S7C) (*19*). This up-regulation correlated with a decreased enrichment of H3K27me3 over class I *KNOX* loci in *h3.1kd* (Fig. 2E and fig. S7, D to F). In addition, class I *KNOX* genes were ectopically expressed in leaves of *h3.1kd* (fig. S7G), consistent with the growth of ectopic leaflets (fig. S5C). Thus, knockdown of *H3.1* compromises deposition of H3K27me3.

Loss of H3K27me3 in *h3.1kd* was not due to misexpression of PcG genes or H3K27 demethylases, nor did it originate from a perturbed cell cycle (fig. S8). To test whether the lack of H3.1 as a substrate for trimethylation at K27 caused impaired H3K27me3 maintenance, we created point-mutated H3.1K4A, H3.1K9A, and H3.1K27A (A, alanine). Only H3.1K27A failed to rescue the developmental defects, reduction of H3K27me3 levels, and derepression of class I *KNOX* genes in *h3.1kd-1* (Fig. 2F and fig. S9, A to C), suggesting the importance of H3.1 as a substrate for inheritance of H3K27me3. PRC2 does not prefer H3.1 over H3.3 as a substrate (*15*, *20*), and H3.1 and H3.3 carry comparable levels of H3K27me3 in *Arabidopsis* (fig. S9D). Four residues at positions 31, 41, 87, and 90 distinguish H3.1 from H3.3, but A31 alone confers the specificity of H3.1 monomethylation by ATXR5/6 (fig. S9E) (*15*). We mutated each of the four amino acids in H3.1 to the corresponding H3.3 amino acid. Only the mutation A31T (Ala^{31}→Thr^{31}) failed to rescue the developmental defects and the reduction of H3K27me3 levels in *h3.1kd-1* (Fig. 2F and fig. S9, F and G), suggesting that monomethylation of K27 on H3.1 is responsible for maintenance of H3K27me3. The degree of reduction of H3K27me3 levels in *h3.1kd* lines was correlated with the enrichment of H3K27me1 in the wild type (fig. S10A). Moreover, a moderate global loss of H3K27me1 in a hypomorphic *atxr5;atxr6* mutant reduced H3K27me3 enrichment at genes most deprived of H3K27me3 in *h3.1kd* lines (fig. S10, B to D) (*16*). Together, these results suggest that in the context of the replication fork, ATXR5/6 selectively monomethylates K27 of H3.1 and provides H3K27me1 as a substrate for rapid methylation by PRC2 to generate H3K27me3.

To further understand the connection between H3.1-dependent H3K27me3 propagation and the inheritance of the memory of silencing during DNA replication, we engineered an inducible knockdown of *H3.1* by triggering the expression of *amiRHTR13-1* in the *htr1;htr2;htr3;htr9* mutant upon dexamethasone (DEX) treatment (Fig. 3, A and B). To monitor the impact of the treatment, we examined transcript levels of *AT5G60250* and *AT5G60610* because these genes showed a strong loss of H3K27me3 and concomitant up-regulation in *h3.1kd* lines (Fig. 2, D and E, and fig. S7, D to F). *HTR13* transcript levels were reduced after DEX treatment for 48 hours, but reduction of H3K27me3 and up-regulation of *AT5G60250* and *AT5G60610* only took place at 96 hours (Fig. 3, C and D). The cell cycle duration in *Arabidopsis* ranges from 17 to 48 hours (*21*, *22*), suggesting that, upon the loss of H3.1, dilution of H3K27me3 levels by at least one or two cycles of DNA replication causes transcriptional activation. Inhibition of DNA replication by olomoucine or roscovitine (*23*) (Fig. 3B and fig. S11) blocked DEX-induced loss of

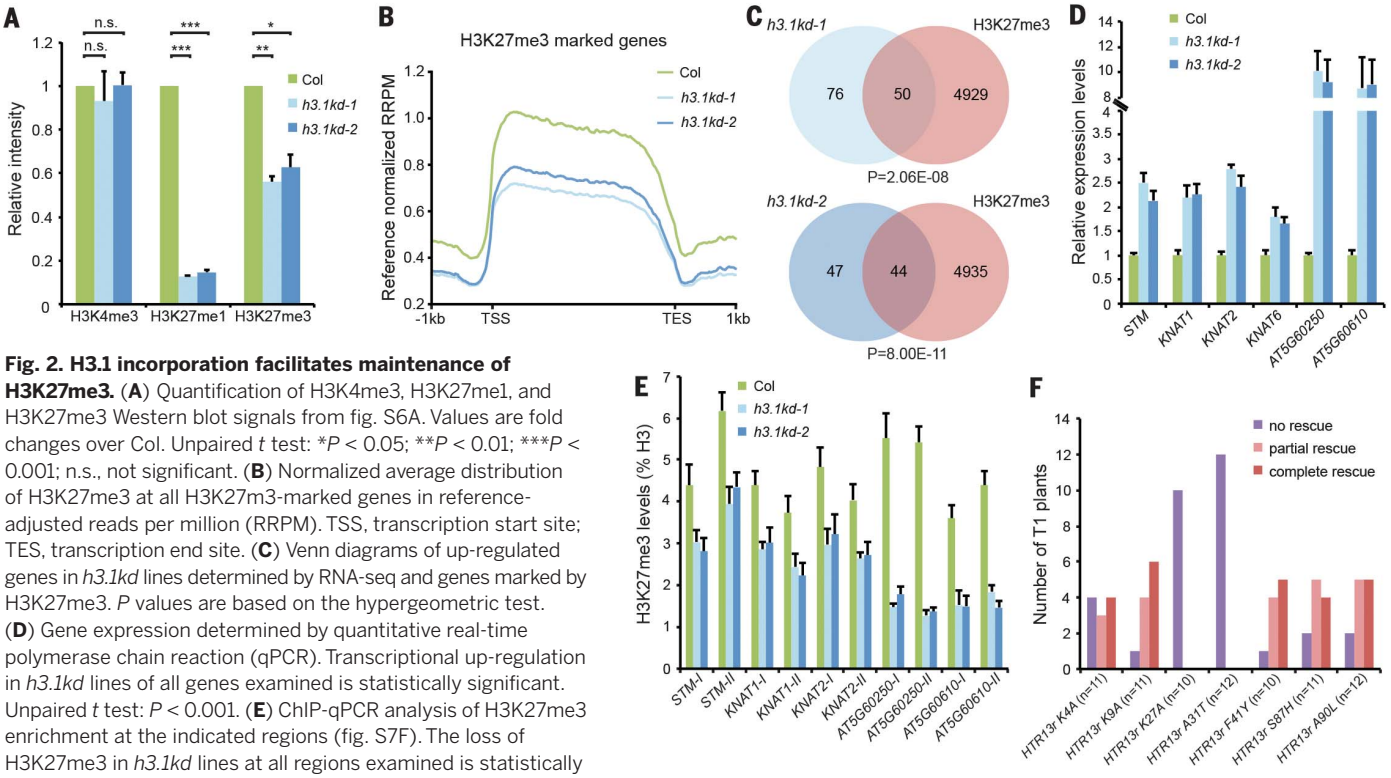

Fig. 2. H3.1 incorporation facilitates maintenance of H3K27me3. (**A**) Quantification of H3K4me3, H3K27me1, and H3K27me3 Western blot signals from fig. S6A. Values are fold changes over Col. Unpaired *t* test: **P* < 0.05; ***P* < 0.01; ****P* < 0.001; n.s., not significant. (**B**) Normalized average distribution of H3K27me3 at all H3K27m3-marked genes in reference-adjusted reads per million (RRPM). TSS, transcription start site; TES, transcription end site. (**C**) Venn diagrams of up-regulated genes in *h3.1kd* lines determined by RNA-seq and genes marked by H3K27me3. *P* values are based on the hypergeometric test. (**D**) Gene expression determined by quantitative real-time polymerase chain reaction (qPCR). Transcriptional up-regulation in *h3.1kd* lines of all genes examined is statistically significant. Unpaired *t* test: *P* < 0.001. (**E**) ChIP-qPCR analysis of H3K27me3 enrichment at the indicated regions (fig. S7F). The loss of H3K27me3 in *h3.1kd* lines at all regions examined is statistically significant. Unpaired *t* test: *P* < 0.001. (**F**) Number of T1 transgenic plants that showed no rescue, partial rescue, and complete rescue of the *h3.1kd-1* phenotype, as defined in fig. S5E. The number (*n*) of T1 plants analyzed for each construct is indicated. For all experiments, error bars represent SD from three biological replicates.

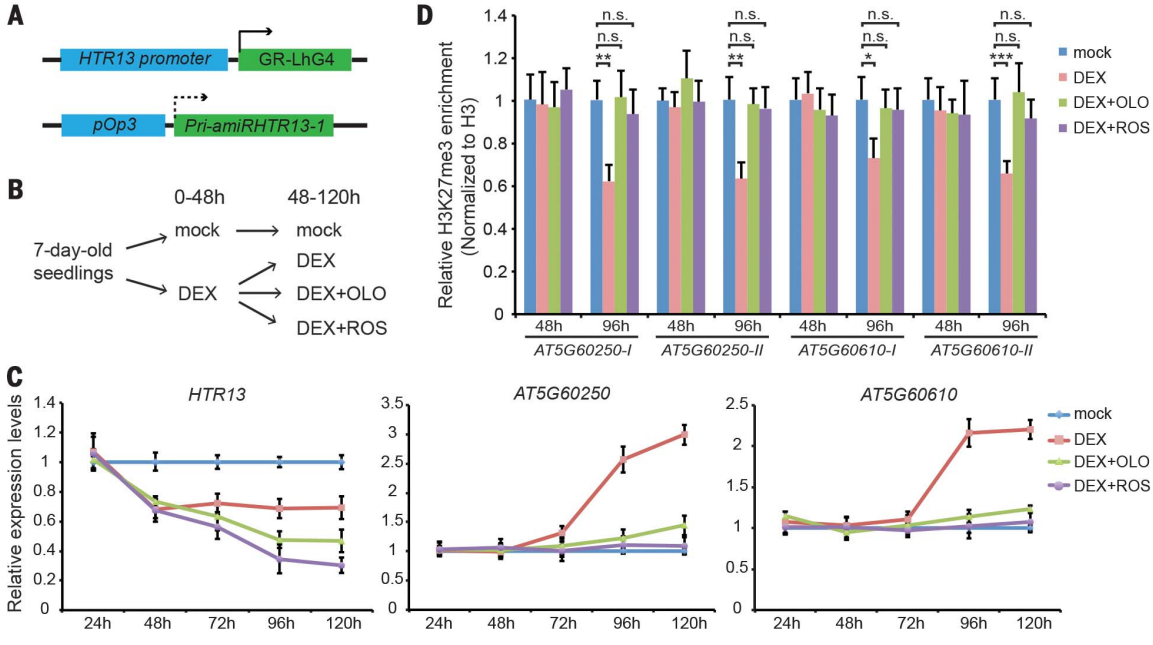

Fig. 3. H3.1-dependent propagation of H3K27me3 maintains the memory of silencing during DNA replication. (**A**) GR-LhG4 expressed under the control of the *HTR13* promoter (solid arrow) can be activated by DEX and subsequently binds to the *pOp3* promoter to activate *amiRHTR13-1* transcription (dashed arrow). (**B**) Experimental design of treatment with DEX and the cell cycle inhibitors olomoucine (OLO) and roscovitine (ROS). (**C**) Gene expression upon DEX and cell cycle inhibitor treatment. (**D**) Relative H3K27me3 levels at *AT5G60250* and *AT5G60610* chromatin in seedlings treated with DEX and cell cycle inhibitors. For all experiments, error bars represent SD from three biological replicates. Unpaired *t* test: $*P < 0.05$; $**P < 0.01$; $***P < 0.001$; n.s., not significant.

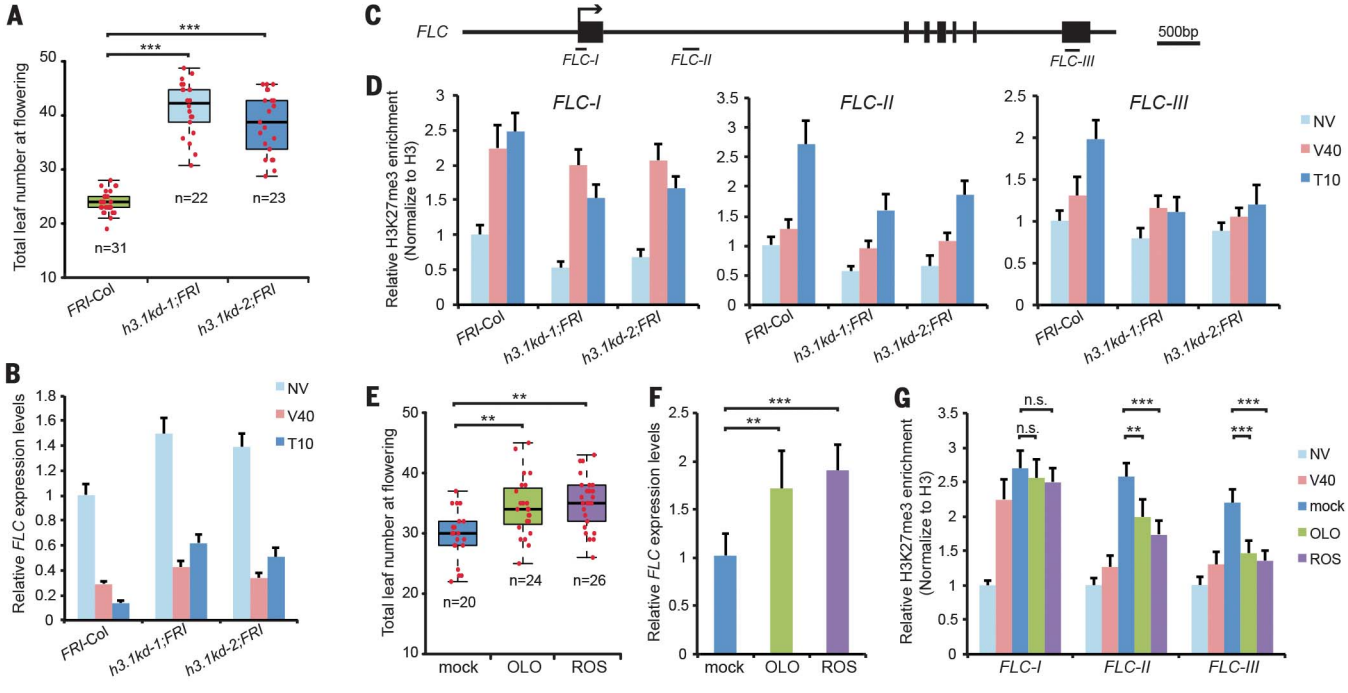

Fig. 4. Replication-dependent H3.1 deposition facilitates H3K27me3 enrichment at *FLC* by vernalization. (**A**) Flowering time after vernalization. The number (*n*) of plants counted for each line is indicated. (**B**) *FLC* transcript levels in *FRI*-Col and *h3.1kd* lines. NV, no vernalization; V40, 40-day cold treatment; T10, 40-day cold treatment followed by 10-day growth at warm temperatures. Error bars represent SD from three biological replicates. (**C**) Schematic view of the *FLC* gene structure, indicating regions examined by ChIP-qPCR. Black boxes represent exons, and lines represent intergenic regions and introns. The arrow indicates the TSS. bp, base pairs. (**D**) Relative H3K27me3 levels at *FLC* during vernalization. Error bars represent SD from three biological replicates. (**E**) Flowering time of cell cycle inhibitor–treated plants. The number of plants counted for each line is indicated. (**F**) *FLC* transcript levels in cell cycle inhibitor–treated seedlings. Error bars represent SD from three biological replicates. (**G**) Relative H3K27me3 enrichment at *FLC* in cell cycle inhibitor–treated seedlings. Error bars represent SD from three biological replicates. For all experiments, unpaired *t* test: $**P < 0.01$; $***P < 0.001$; n.s., not significant.

H3K27me3 and gene activation (Fig. 3, C and D). Together, these results indicate that replication-coupled propagation of H3K27me3 on H3.1 is required to maintain the memory of silencing during DNA replication (fig. S12).

We further investigated the establishment of H3K27me3-mediated silencing in the context of flowering, the transition from vegetative growth to reproductive growth. Vernalization, a prolonged cold treatment, induces H3K27me3 enrichment that stably silences the flowering repressor *FLC* (*FLOWERING LOCUS C*) (*24*). H3K27me3 enrichment is induced at the nucleation region around the transcription start site (TSS) of *FLC* at low temperatures, from where it spreads to the *FLC* gene body during subsequent growth in warm temperatures and is retained as the epigenetic memory of vernalization (*24*). We introduced a functional *FRI* (*FRIGIDA*) allele, which confers a requirement for vernalization to accelerate flowering, into *h3.1kd* lines. After vernalization, flowering was delayed in *h3.1kd* lines (Fig. 4A and fig. S13A), and *FLC* expression increased (Fig. 4B). Cold-induced nucleation of H3K27me3 was observed at the TSS of *FLC* in *h3.1kd*, but H3K27me3 maintenance and spreading over *FLC* was impaired (Fig. 4, C and D, and fig. S13B). During vernalization, H3.3 enrichment at *FLC* decreased, whereas H3.1 enrichment increased and balanced total H3 levels (fig. S13, B and C). In contrast to seedlings, mature *Arabidopsis* leaves that are devoid of replicating cells had impaired H3K27me3 enrichment after vernalization (*25*), and H3.1 did not increase in response to vernalization (fig. S13, D and E). To address the link between H3.1, DNA replication, and spreading of H3K27me3, we impeded cell cycle progression after cold exposure (fig. S14A). Plants treated with cell cycle inhibitors flowered later than untreated plants (Fig. 4E and fig. S14B), showed higher *FLC* expression levels (Fig. 4F), and reduced spreading of H3K27me3 at *FLC* (Fig. 4G and fig. S14C). Together, these data demonstrate that H3.1 deposition by DNA replication facilitates establishment of H3K27me3 at *FLC* chromatin during vernalization, although spreading of H3K27me3 at *FLC* might be independent from maintenance of H3K27me3 at the initial nucleation site (fig. S14D).

We demonstrate that plant-specific monomethylation of H3.1 and tethering of PcG proteins to the replication fork restores H3K27me3 to maintain the memory of silencing. Similarly, DNA replication has been implicated in the silencing of heterochromatin by facilitating the propagation of H3K9 methylation in fission yeast (*26*, *27*). In the context of postembryonic development, plants also evolved a mechanism that evicts PcG proteins from the chromatin and dilutes H3K27me3 in a cell cycle–dependent manner during plant cell fate determination (*28*). In contrast with that of most animals, plant development is largely postembryonic and plastic. The mechanism reported in this study enables plant cells to face a high potential of regeneration and loss of cell fate. Hence, engineering of the epigenetic memory of silencing in a replication-coupled manner might allow manipulation of developmental plasticity and regeneration in eukaryotes.

REFERENCES AND NOTES

1. D. M. MacAlpine, G. Almouzni, *Cold Spring Harb. Perspect. Biol.* **5**, a010207 (2013).
2. K. Ahmad, S. Henikoff, *Mol. Cell* **9**, 1191–1200 (2002).
3. H. Tagami, D. Ray-Gallet, G. Almouzni, Y. Nakatani, *Cell* **116**, 51–61 (2004).
4. J. A. Simon, R. E. Kingston, *Nat. Rev. Mol. Cell Biol.* **10**, 697–708 (2009).
5. J. Xiao, D. Wagner, *Curr. Opin. Plant Biol.* **23**, 15–24 (2015).
6. F. Laprell, K. Finkl, J. Müller, *Science* **356**, 85–88 (2017).
7. R. T. Coleman, G. Struhl, *Science* **356**, eaai8236 (2017).
8. R. Margueron *et al.*, *Nature* **461**, 762–767 (2009).
9. K. H. Hansen *et al.*, *Nat. Cell Biol.* **10**, 1291–1300 (2008).
10. C. Alabert *et al.*, *Genes Dev.* **29**, 585–590 (2015).
11. A. N. Scharf, T. K. Barth, A. Imhof, *Nucleic Acids Res.* **37**, 5032–5040 (2009).
12. M. Xu, W. Wang, S. Chen, B. Zhu, *EMBO Rep.* **13**, 60–67 (2012).
13. A. Ebert *et al.*, *Genes Dev.* **18**, 2973–2983 (2004).
14. K. J. Ferrari *et al.*, *Mol. Cell* **53**, 49–62 (2014).
15. Y. Jacob *et al.*, *Science* **343**, 1249–1253 (2014).
16. Y. Jacob *et al.*, *Nat. Struct. Mol. Biol.* **16**, 763–768 (2009).
17. D. A. Orlando *et al.*, *Cell Reports* **9**, 1163–1170 (2014).
18. X. Zhang *et al.*, *PLOS Biol.* **5**, e129 (2007).
19. S. Scofield, J. A. Murray, *Plant Mol. Biol.* **60**, 929–946 (2006).
20. L. A. Banaszynski *et al.*, *Cell* **155**, 107–120 (2013).
21. K. Hayashi, J. Hasegawa, S. Matsunaga, *Sci. Rep.* **3**, 2723 (2013).
22. G. V. Reddy, M. G. Heisler, D. W. Ehrhardt, E. M. Meyerowitz, *Development* **131**, 4225–4237 (2004).
23. S. Planchais, N. Glab, D. Inzé, C. Bergounioux, *FEBS Lett.* **476**, 78–83 (2000).
24. J. Song, J. Irwin, C. Dean, *Curr. Biol.* **23**, R807–R811 (2013).
25. E. J. Finnegan, E. S. Dennis, *Curr. Biol.* **17**, 1978–1983 (2007).
26. F. Li, R. Martienssen, W. Z. Cande, *Nature* **475**, 244–248 (2011).
27. M. Zaratiegui *et al.*, *Nature* **479**, 135–138 (2011).
28. B. Sun *et al.*, *Science* **343**, 1248559 (2014).

ACKNOWLEDGMENTS

We thank S. Akimcheva for assistance with BY-2 cell culture; B. Lei for providing HEK293 cells; M. Goiser for help with bioinformatics; and O. Bell, I. Drinnenberg, M. Borg, and J. M. Watson for critical reading of the manuscript. D.J. was supported by the European Molecular Biology Organization long-term fellowship (ALTF 1129-2013). This work was supported by grant P28320-B21 from the Austrian Science Fund (FWF), core funding from the Gregor Mendel Institute, the Vienna Biocenter Core Facilities for Next Generation Sequencing and Plant Science, and the IMP/IMBA BioOptics Facility. The supplementary materials contain additional data. The sequencing data generated in this study are deposited at the Gene Expression Omnibus (accession number GSE101221).

SUPPLEMENTARY MATERIALS

www.sciencemag.org/content/357/6356/1146/suppl/DC1
Materials and Methods
Figs. S1 to S14
Tables S1 and S2
References (*29*–*51*)

21 April 2017; accepted 9 August 2017
Published online 17 August 2017
10.1126/science.aan4965

Science

DNA replication–coupled histone modification maintains Polycomb gene silencing in plants

Danhua Jiang and Frédéric Berger

Science **357** (6356), 1146-1149.
DOI: 10.1126/science.aan4965originally published online August 17, 2017

Managing gene silencing through replication

Vernalization is the process in plants by which wintertime chill stimulates springtime flowering. Yang *et al.* and Jiang and Berger show how chill is recorded in *Arabidopsis* epigenetically by methylation of histones. Specialized components of the Polycomb group of proteins remodel DNA to establish the methylation marks and are linked to DNA replication. Long-term stable epigenetic status follows rapid establishment of metastable epigenetic marks. This epigenetic strategy may be key to the developmental requirement of both secure and nimble fate decisions, allowing plant cells to change fates.

Science, this issue p. 1142 and p. 1146

Science (print ISSN 0036-8075; online ISSN 1095-9203) is published by the American Association for the Advancement of Science, 1200 New York Avenue NW, Washington, DC 20005. The title *Science* is a registered trademark of AAAS.